ABOVEGROUND BIOMASS ESTIMATION USING AIRBORNE LASER SCANNING (ALS) AND STRUCTURE FROM MOTION (SFM) IN TROPICAL MONTANE FOREST, NORTHERN BORNEO

Wilson V. C. Wong[1,2a], Satoshi Tsuyuki[2b] , Mui-How Phua[1c], Keiko Ioki[1d], Alexius Korom[1e], Yasumasa Hirata[3f], Hideki Saito[3g], Gen Takao[3h]

[1]Faculty of Science and Natural Resource, Universiti Malaysia Sabah, Locked bag 2073, 88999 Kota Kinabalu, Sabah, Malaysia,

Email: [a]w.wilson@ums.edu.my, [c]pmh@ums.edu.my, [d]keiko_ioki@ums.edu.my, [e]alexi502@sabah.uitm.edu.my

[2]Graduate School of Agricultural and Life Sciences, The University of Tokyo, 1-1-1 Yayoi, Bunkyo-Ku, Tokyo 113-8657, Japan,

Email: [b]tsuyuki@fr.a.u-tokyo.ac.jp

[3]Forestry and Forest Products Research Institute, Matsunosato 1, Tsukuba, Ibaraki 305-8687, Japan,

Email: [f]hirat09@affrc.go.jp, [g]rslsaito@ffpri.affrc.go.jp, [h]takaogen@affrc.go.jp

KEY WORDS: Structure from motion, airborne laser scanning, aboveground biomass, tropical montane forest

ABSTRACT: The advancement technology of airborne laser scanning (ALS) and structure from motion (SfM) offer high capability in forest assessment such as aboveground biomass (AGB) estimation. In this study, we compared the capability of ALS and SfM datasets in estimating AGB for tropical montane forest, North Borneo. ALS and SfM datasets were acquired using Riegl-LMS Q560 sensor and digital single lens reflex (DSLR) camera of Canon 1D Mark III, respectively. SfM dataset was derived by processing the aerial photographs using Agisoft PhotoScan Pro software. We used 45 plots collected in the field and the predictor variables derived from ALS and SfM datasets to develop the AGB models by using multiplicative linear regression. Relative mean square error (RMSE) was found slightly lower in AGB estimation using ALS dataset (RMSE=89.38 Mg/ha; RMSE%=32.41%; R^2=0.7923) compared to SfM dataset (RMSE=96.75 Mg/ha; RMSE%=35.09%; R^2=0.7442) with the value of 2.68%. The result demonstrated that SfM dataset can be utilized for AGB estimation given the availability of aerial photographs and digital terrain model (DTM) derived from ALS.

1. INTRODUCTION

Global warming is now ninety-five percent certain caused by human activities (IPCC, 2014) and stabilizing temperature increase will require commitment from the global community. The most visible evidence is the decrease in the annual mean ice extent cover in artic region in the range of 3.5 to 4.1% per decade between the period of 1979 (after the satellite observations initiated) to 2012 and the global mean sea level rose by 19 ±2 cm over the period of 1901 to 2010. In the IPCC's Fifth Assessment Report (AR5), scientific analysis showed that the total anthropogenic greenhouse gases (GHG) emissions have continued to increase over 1970 to 2010 and aggravated for the period between 2000 to 2010 with total GHG emissions in 2010 reached 49 $GtCO_2$ -eq/yr, almost twice the amount in 1970 (i.e. 27 $GtCO_2$ -eq/yr). Carbon dioxide emitted from forestry and other land use (FOLU) was estimated at 5.4 $GtCO_2$ -eq/yr in 2010 or approximately 11% of the total GHG emissions for that year (IPCC, 2014).

Kyoto Protocol provided no opportunity for the engagement among developing countries which reduce emission through reducing deforestation rates. Recognizing the importance of developing countries along with industrialized countries for the total emission reduction from all major sources, the timely proposal of reducing emission from deforestation was presented by the government of Costa Rica and Papua New Guinea during the 11th session of Conference of Parties (COP) to the United Nations Framework Convention on Climate Change (UNFCCC) in Montreal, 2005 (UNFCCC, 2005).Two years later in COP 13, the proposal of "reducing emissions from deforestation in developing countries: approaches to stimulate action" was adopted in Decision 2/CP.13. In the same COP 13, recognizing the important of co-benefits of protecting forest carbon, the REDD was further developed to REDD-plus (reducing emissions from deforestation and forest degradation and the role of conservation, sustainable management of forests an enhancement of forest carbon stocks in developing countries) which was adopted as part of the Bali Action Plan (Decision 1/CP.13) (UNFCCC, 2007). SBSTA (Subsidiary Body for Scientific and Technological Advice), one of the permanent subsidiary bodies to the Convention established by the COP/CMP, was assigned to address many scientific and technical issues related to the REDD-plus. Remote sensing technology with combination of ground-based forest carbon inventory approaches for estimating forest carbon stocks and forest area changes was accepted in the methodological guidance for activities relating to REDD-plus which contribute to the robust and transparent forest monitoring system or known as MRV (measurement, reporting and verification) system (Decision 4/CP. 15). MRV's main objective is to estimate and report the national-scale forest emissions and removals based on

the three main components (1) satellite land monitoring system, (2) the national forest Inventory, and (3) the national GHG inventory (UN-REDD, 2013) which contribute to the robust national monitoring system with data and information that are transparent, consistent over time, and are suitable for the measuring, reporting and verifying anthropogenic forest-related emissions by sources and removals by sinks, forest carbon stocks, and forest carbon stock and forest-area changes (Decision 11/ CP. 19).

Remote sensing dataset varied in terms of the type of information and accuracy depending on the sensor type and altitude or distance from the land surface. Basically, categorization can be grouped by sensor type (i.e. optical, LiDAR or SAR) or platform (i.e. space-borne or airborne). Application in forest biomass estimation have been attempted using variety of remote sensing dataset of optical system (e.g. Hirata et al., 2014; Phua and Saito, 2008), airborne laser scanning (ALS) (e.g. Ioki et al., 2014; Fassnacht et al., 2015) and Synthetic Aperture Radar (SAR) (e.g. Dobson et al., 1992). The limited use of space-borne dataset is largely due to cloud cover and poor correlation between spectral information and biomass especially in high biomass of forest (Koch, 2010). The cloud cover for tropic area was estimated at 58 to 70% according to the International Satellite Cloud Climatology Project (ISCCP). Space-borne LiDAR such as the ICESat/GLAS with large footprint of 70 m was still limited due to the laser spots separated by nearly 170 m along the satellite's ground track while the space-borne radar faced by saturation problem (Koch, 2010). Height information which derived from the airborne platform has been demonstrated to be superior in estimating forest variables related to height such as volume, tree height and biomass (e.g. Nurminen et al., 2013; Rahfl et al., 2014; Vastaranta et al., 2013). Among the type of remote sensing dataset, airborne laser scanner (ALS) dataset was found to rank first, followed by SfM dataset, interferometry SAR and radargrammetry in estimating stem volume (e.g. Rahfl et al., 2014).

Technical issues related to REDD-plus are still undergoing continuous technical development especially on finding the cost effective method and producing high accuracy forest biomass estimation in the diverse forest types and ecosystems. Estimation of aboveground biomass using ALS dataset have demonstrated to be superior in estimating forest variables. However, in recent time, the development of digital photogrammetry or also known as structure from motion (SfM) is capable to produce dense three-dimensional points in full automation, thus provide a potential opportunity especially in forest monitoring application due to its main advantage of relatively low cost data acquisition compared to ALS dataset (e.g. Leberl et al., 2010). Continuous comparative studies (e.g. using different predictive method, number of ground samples and type of remote sensing dataset) is needed to establish robust best-practice recommendations for improving both regional and global biomass estimates using remote sensing dataset (Fassnacht et al., 2014). Aerial photographs are potentially cost-effective approach for monitoring aboveground biomass given the availability of regular flight mission of aerial photographs acquisition in addition to the availability of digital terrain model from ALS. In this study, we evaluated and compared aboveground biomass estimated using ALS and SfM datasets in tropical montane forest environment.

2. MATERIALS AND METHODS

2.1. Study site

The study area is located in Ulu Padas forest area (approximately 4°27' N, 115°44' E; Figure 1) of Northern Borneo, Malaysia, inside the Heart of Borneo initiative area which forms part of an important mountain eco-regional representation of Borneo together with Pulong Tau National park in Sarawak and Kayan Mentarang National Park in Kalimantan, Indonesia. The study area is compounded by site 1 (Figure 1), approximately 2,000 hectare, of the flight mission of LiDAR and aerial photographs data acquisition in October 2012. The elevation ranges from 961 meter to 1,895 meter with slope average of 18.6°, and generally covered by vegetation with mean canopy height of 22.5 m with SD of 9.0 m (information is derived by using ALS dataset; see Wong et al., 2014). The vegetation of this region consists of several types (i.e. dominant montane oak/chestnut forest with *Agathis*, hill dipterocarp forest, stunted montane mossy forest and high-level swamp forest; SBCP (1998)). The land use consists of both small and big scale logging activities by local people and timber companies as well as small scale farming activities by the local people with some portion remaining as old growth forest with the canopy height reaching up to 60 m. Approximately half of the study area is designated as state land where local people of Long Mio have customary access to cultivate the land for their livelihood whereas the remaining is designated as Class II Commercial Forest Reserve (production forest) under the management of Sabah Forest Industries (SFI) as the concessionaire (Figure 1).

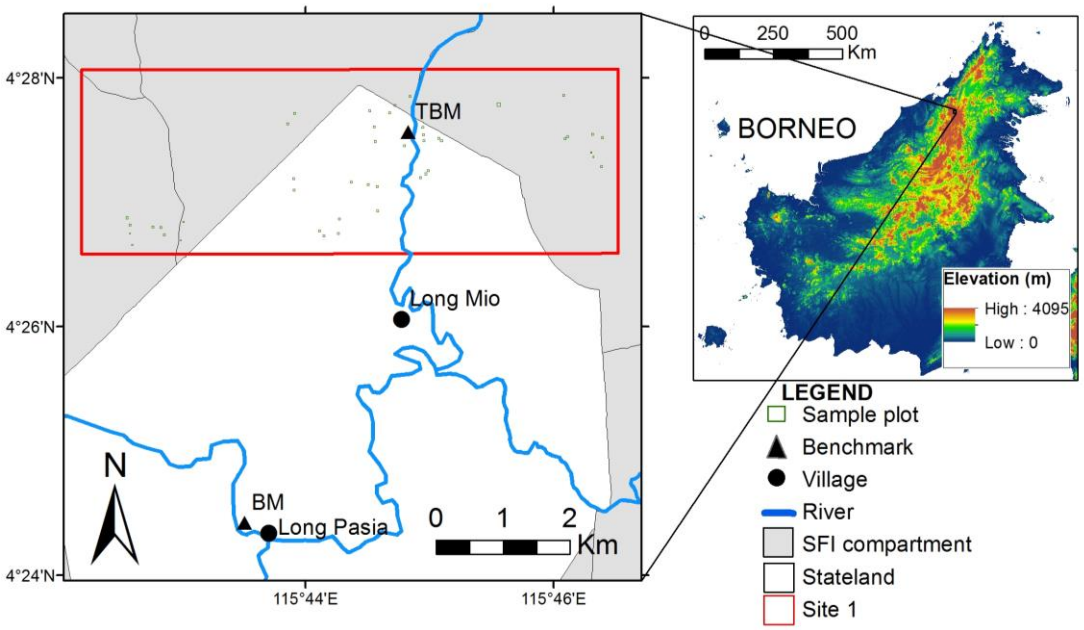

Figure 1: The location of the study area. (Source of elevation data: Shuttle Radar Topography Mission).

2.2. Field data

Field data consisted of individual tree information which was collected between 2011 and 2014. We used 45 plots located in site 1, with each plot size of 900 m^2 (30 m × 30 m; *n*=39) or 400 m^2 (20 m × 20 m; *n*=6). The position of each individual plot was determined using DGNSS (differential global navigation satellite system) receivers of Ashtech ProMark 100 (Spectra Precision, Westminster, CO, USA) and JAVAD Triumph-1 (JAVAD GNSS Inc., CA, USA). Diameter at breast height (DBH) and tree height information were collected for all individual trees with DBH≥10 cm inside the plot area (Table 1). Tree height was measured using electronic hypsometer of TruPulse® 360 Laser RangeFinder with foliage filter (Laser Technology Inc., Colorado, USA) or Haglöf Vertex IV (Haglöf Sweden AB, Västernorrland, Sweden). More than 300 species were recorded such as *Bischofia* sp. (Euphorbiaceae), *Trema* sp. (Ulmaceae), *Lithocarpus* sp. (Fagaceae), *Litsea* sp. (Lauraceae) and *Tristaniopsis* sp. (Myrtaceae).

We used allometric equation of Yamakura et al. (1986) to calculate the biomass for each individual tree using the DBH and tree height information. The biomass per tree was calculated by summing up the stem dry weight per tree (w_s), branch dry weight (w_B) and leaf dry weight (w_L).The equations are as follows;

$$w_s = 2.903 \times 10^{-2}(DBH^2H)^{0.9813} \quad (1)$$

$$w_B = 0.1192\ (w_S)^{1.059} \quad (2)$$

$$w_L = 9.146 \times 10^{-2}(w_S + w_B)^{0.7266} \quad (3)$$

where DBH is the diameter at breast height in cm, H is the total tree height in m.

Then, the biomass for all individual trees within the plot were summed up and converted to the unit of Mg/ha by dividing the value with the plot size (in square meter) and multiply with 10,000. The statistical summary of the AGB estimation was presented in Table 1.

Table 1: Statistics of plots summary of DBH, basal area, tree density and AGB (*n*=45)

	Min	Max	Avg	SD
Mean DBH (*D*), cm	12.80	28.53	19.90	4.29
Basal Area (*G*), m^2/ha	8.94	68.62	29.61	13.08
Tree density (*N*), ha^{-1}	300	1456	750	271
AGB (Mg/ha)	37.98	831.95	275.77	179.93

2.3. ALS dataset

The ALS data was acquired from a flight mission in October 2012 using airborne laser scanner Riegl LMSQ560 (Riegl LMS GmbH, Horn, Austria). The ALS system was attached to helicopter platform, Bell 206B3 Jet Ranger Helicopter and the flight mission was conducted in four days with flying altitude of approximately 400 m above ground level. However, due to the terrain ruggedness and also strong wind on the data acquisition days, the pilot had difficulty in maintaining the pre-planned flying altitude of 400 m above ground level during the entire flight mission. The flying altitude above ground level was calculated ranging from as low as 73 m to 791 m with average of 390 m. The system was operated with 45° of field of view and 240 kHz of pulse repetition rate with beam divergence of less than 0.5 mrad. The side overlap were within 30–50%. The processed data were delivered in the coordinate system of WGS84 UTM Zone 50N/ WGS84 ellipsoid, with classification into ground (4.0%) and non-ground (96.0%) returns comprising 832 million point clouds in LAS 1.2 format (for processing information, see Ioki et al., 2014). The average density was 14.9 pulses/m^2 and vertical accuracy (RMSE) of ALS point cloud was estimated within 25 cm.

2.4. SfM Dataset

The aerial photographs were acquired simultaneously in the same flight mission with the ALS acquisition by using small format digital single lens reflex camera (DLSR) Canon EOS-1D Mark III. The camera was fitted with lens of 28 mm focal length and the cross-track field-of-view and along-track field-of-view are 52.9° and 36.6°, respectively. Flying with the average speed of 100 km/h and exposure interval of 3.5 seconds resulted in 55−70% of forward overlap while the side lap was approximately 45%. Camera settings were set with exposure time of 1/2500 s, ISO-speed of 1250, and aperture range from f/1.8 to f/10. A total of 2400 aerial photographs for site 1 were delivered in 24 bit sRGB on large-size format of JPEG (3888 × 2592) with average GSD (ground sampling distance) of approximately 10 cm together with GNSS/IMU data information.

Aerial photographs were processed using digital photogrammetry technique (also referred to structure from motion, SfM) to generate dense photogrammetric point cloud (SfM point cloud). The SfM software used in this study was Agisoft Photoscan Pro 1.0.3 software package (Agisoft LLC, Sankt-Petersburg, RU). The workflow of digital photogrammetry to produce dense photogrammetric point cloud consists of two stages (Agisoft, 2014). The first stage is camera alignment where image matching is executed to create sparse point cloud model by searching common points on photographs as well as position of each photograph, and refines camera calibration parameters. In this process, we used 2400 aerial photographs and the GNSS/IMU data to generate 3,172,874 points covering an area of approximately 2300 hectare in site 1. Out of the 2400 photographs, 2067 or 86.1 % were aligned. The reported average camera location errors for x, y and z were 1.82 m, 0.69 m and 0.55 m, respectively, and total error was 2.03 m .The second stage is building dense point cloud where the Photoscan calculates depth information for each camera to be combined into a single dense point cloud based on the estimated camera positions. The entire area had to be divided into two blocks (approximately 1,000 hectare each) due to the workstation's processing capability limit. The dense point cloud with a total of 935 million points were generated and exported to LAS format in coordinate system of WGS84 UTM Zone 50N/ WGS84 ellipsoid for further processing. The total processing time was approximately 13 hours by using workstation with the following specifications; Intel Core i5-4670 CPU 3.40GHz Processor, 16.0 GB installed memory (RAM), 64-bit OS, and NVIDIA Quadro K2000 GPU.

The whole process were performed in full automation by selecting a combination of built-in parameters. We used the following parameters for stage 1 of camera alignment; high image matching, point limit of 40,000, and with ground control (i.e. GNSS/IMU data), together with optimization of fit aspect, skew transformation coefficient, focal length, principal point coordinates (*cx*, *cy*), radial distortion coefficient (*k1*, *k2*, *k3*), and tangential distortion coefficient (*p1*, *p2*). For stage 2 of point cloud densification, we used the following parameters; quality of high with advanced option of mild. The settings were decided based on the built-in parameters setting evaluation analysis by employing forward sequential selection to determine the best setting to reproduce photogrammetric point cloud in a test area of 100 ha. This is important otherwise even a robust matching method would produce an unsatisfactory three-dimensional reconstruction (Remondino et al., 2014).

2.5. Processing of ALS and SfM datasets

ALS points of single, first and last returns were extracted by filtering the intermediate returns and used in further processing steps. Both the ALS and SfM points were normalised using the ground points of ALS dataset. Then, ALS points and SfM points were extracted for each plot. We used the canopy points height of 2 m and above (i.e. removing the effect of shrubs, stones, etc. (Næsset, 1997)) to compute the predictor variables (e.g. Nurminen et al., 2013) by deriving 16 height variables and 9 canopy cover percentile variables (Figure 2). We used height variables of

maximum (h_{max}), minimum (h_{min}), mean (h_{mean}), standard deviation (h_{std}), percentiles at 10% intervals (h_{10}, h_{20}, …, h_{90}) and percentile at 25% (h_{25}), 75% (h_{75}) and 95% (h_{95}). Canopy cover percentile was computed as the proportion of returns below certain percentage of total height with 10% interval (d_{10}, d_{20}, …, d_{90}). We performed log transformation to all the predictor variables and thus doubled the number of predictor variables.

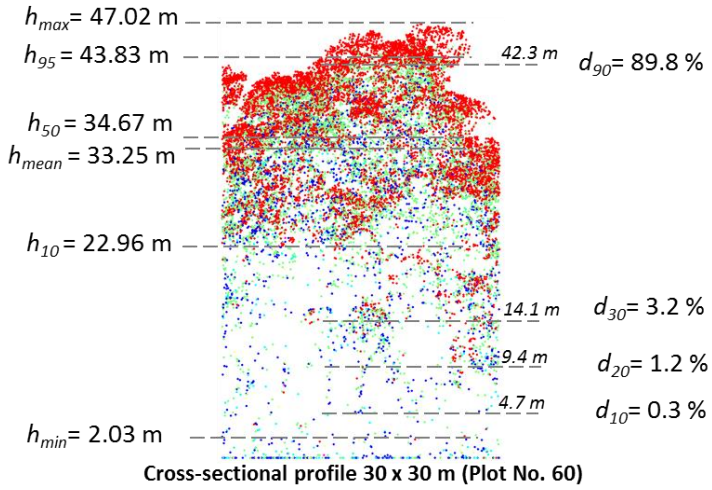

Figure 2: Several predictor variables values of height (left) and canopy cover percentile (right) derive from ALS dataset.

2.6. Prediction method

Forward stepwise linear regression was used for the multiplicative model development. Stepwise linear regression using Akaike information criterion (AIC) to select the final model with lowest AIC value and was performed in R software ver.3.1.0 (R Development Core Team, Vienna, Austria). Multicollinearity of the predictor variables were examined using variance inflation factor (VIF). For each model, stepwise linear regression were performed separetely using four equation types as shown below;

$$AGB = \beta_0 + \beta_1 X_1 + \beta_2 X_2 + \cdots + \beta_n X_n \quad (4)$$

$$AGB = \beta_0 + \beta_1 \mathrm{Ln}(X_1) + \beta_2 \mathrm{Ln}(X_2) + \cdots + \beta_n \mathrm{Ln}(X_n) \quad (5)$$

$$\mathrm{Ln}(AGB) = \beta_0 + \beta_1 X_1 + \beta_2 X_2 + \cdots + \beta_n X_n \quad (6)$$

$$\mathrm{Ln}(AGB) = \beta_0 + \beta_1 \mathrm{Ln}(X_1) + \beta_2 \mathrm{Ln}(X_2) + \cdots + \beta_n \mathrm{Ln}(X_n) \quad (7)$$

where AGB is the response variable of aboveground biomass, β is the coefficient and X is the predictor variables.

Cross-validation was performed to assess the accuracy of the AGB estimation using leave-one-out-cross-validation (LOOCV). LOOCV technique requires one of the training plots to be removed from the dataset at a time, while the remaining plots (n-1) to be fitted using the selected model of AGB. The estimated AGB were then predicted for the removed plot. This procedure was repeated until all estimated values were obtained for all plots. The accuracy of the estimations was assessed by the root mean square error (RMSE) and relative RMSE (RMSE%) using the original scale values:

$$Root\ Mean\ Square\ Error\ (RMSE) = \sqrt{\frac{1}{n}\sum_{i=1}^{n}(y_i - \hat{y}_i)^2} \quad (8)$$

$$Relative\ Root\ Mean\ Square\ Error\ (RMSE\%) = 100 \times \frac{RMSE}{\bar{y}} \quad (9)$$

where y_i is the surveyed reference value for plot i, $\hat{y}_i$ is the remote-sensing based prediction, $\bar{y}$ is the arithmetic mean of the surveyed aboveground biomass, n is the number of the plot.

3. RESULTS

Stepwise linear regression was employed in estimating aboveground biomass using both ALS and SfM datasets. In the AGB estimation using ALS dataset, a combination of height variable (i.e. h_{60}) and canopy cover percentile variables (i.e. d_{10} and d_{70}) yielded RMSE and RMSE% values of 89.38 Mg/ha and 32.41%, respectively (Table 2). AGB estimation using SfM dataset yielded slightly higher RMSE and RMSE% values of 96.75 Mg/ha and 35.09%, respectively. By comparing the RMSE values separately in 4 equation types instead of selecting the model based on the highest R^2, using a combination of AGB as response variable and h_{60} as predictor variable reduced the RMSE values by 28.47 Mg/ha compared to variable combination of Ln(AGB) and h_{60} (i.e. highest R^2) (Table 2). The average VIF values were not exceed more than 2 and it was suggested that there were no severe multicollinearity between variables for each model (e.g. Eckert, 2012; Thapa et al., 2015). However, negative value of AGB of approximately 100 Mg/ha was observed in Bukit Rimau area, occurred in one plot using ALS dataset and two plots using SfM dataset. ALS dataset was found to be slightly superior compared to SfM dataset in estimating AGB with lower values of RMSE and RMSE% values by 7.37 Mg/ha and 2.68%, respectively. The R^2 value when using ALS dataset was found to be slightly higher in comparison to SfM dataset by 0.048.

Table 2: Multiplicative model of AGB estimation using ALS and SfM dataset (n=45).

MODELS	RMSE	RMSE%	R^2	VIF	AIC
ALS					
$AGB=24.866*(h_{60})-49.279*(d_{10})+2.192*(d_{70})-365.517$	**89.38**	**32.41**	**0.7923**	**1.801**	**404.59**
$AGB=342.925*\mathrm{Ln}(h_{mean})-36.823*\mathrm{Ln}(d_{20})-681.095$	124.20	45.04	0.6348	1.070	428.00
$\mathrm{Ln}(AGB)=0.09167*(h_{60})+0.02696*(d_{90})+0.8108$	146.93	53.28	0.7783	1.596	-92.09
$\mathrm{Ln}(AGB)=1.5967*\mathrm{Ln}(h_{60})+0.5644$	93.21	33.80	0.7591	1.000	-90.35
SfM					
$AGB=19.643*(h_{50})-168.599$	**96.75**	**35.09**	**0.7442**	**1.000**	**409.98**
$AGB=271.459*\mathrm{Ln}(h_{50})-521.994*\mathrm{Ln}(d_{90})+1804.30$	131.40	47.65	0.6182	1.550	430.00
$\mathrm{Ln}(AGB)=0.0758*(h_{60})+3.603$	125.22	45.41	0.7486	1.000	-88.43
$\mathrm{Ln}(AGB)=1.4846*\mathrm{Ln}(h_{60})+0.0806$	98.17	35.60	0.7213	1.000	-83.79

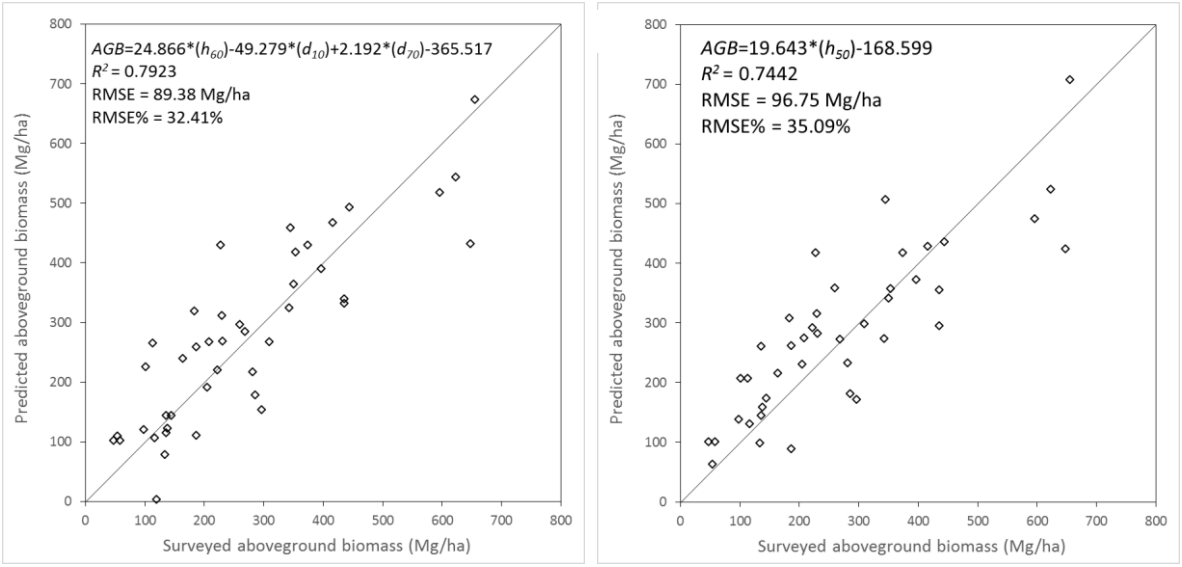

Figure 3: Scatter plots of predicted AGB versus surveyed AGB using multiplicative model using ALS dataset (left) and SfM dataset (right).

4. DISCUSSION

The recent development in digital photogrammetry technology enables the full automation in deriving three-dimensional dataset in a dense point-cloud form, or also known as Structure from Motion (SfM). In the previous photogrammetry technology of analytical photogrammetry, three dimensional dataset can be derived manually in digital form and it has been used with success in forestry applications (e.g. Fujita et al., 2003; Okuda et al., 2004). However the major drawback of analytical photogrammetry is its limited capability to cover large areas of forest where height must be manually digitized – on a typical grid of 2.5 to 5 m and typically limited to 10 to 100 ha. For example, Okuda et al. (2004) estimated AGB using mean canopy surface height derived by using analytical photogrammetry technique in a 2.5 m grid system for a 56-ha tropical rainforest. In this study, we generated highly dense point cloud, approximately 935 million points covering 2,000 ha using SfM approach. The advancement of GNSS/IMU has decreased the need for ground-control points in areas where it is not feasible to collect them, such as in forest environment.

There is lack of studies using both ALS and SfM datasets for forestry applications in tropical rainforest environment (e.g. Wong et al. 2015). Many of previous studies using both ALS and SfM datasets were performed in temperate forest or boreal forest and evaluating forest biophysical characteristics such as stem volume, tree height, basal area, diameter and tree density (e.g. Bohlin et al. 2012; Gobakken et al. 2015; Rahfl et al. 2014; Vastaranta et al. 2013). Wong et al. (2015) evaluated forest biophysical characteristics (i.e. tree height, diameter, basal area and tree density) using both ALS and SfM datasets in the same study area. In those findings, ALS dataset generally was found to be only slightly superior compared to SfM dataset in estimating those forest biophysical characteristics where only small differences in performance were observed. In certain instances, SfM can be found to be slightly better than ALS (e.g. Gobakken et al. 2015). A study conducted in seasonal tropical forest in Cambodia by Ota et al. (2015) demonstrated the difference of RMSE value at 0.35 Mg/ha when compared the estimation using ALS (RMSE=29.12 Mg/ha) and SfM (RMSE=29.47 Mg/ha) datasets. In this study, the difference of relative RMSE values for AGB estimation using ALS and SfM was 2.68%.

Derivation of SfM dataset from aerial photographs depends on several factors: (1) image-matching algorithm (e.g. Remondino et al. 2014), (2) type of camera/ sensor (e.g. Müller et al. 2014), (3) camera and flight parameter settings (e.g. Agisoft, 2014), (4) overlap rate (e.g. Nurminen et al. 2013), (5) environmental conditions (e.g. Nex and Remondino, 2014), and (6) object characteristics (e.g. Remondino et al. 2014). A combination of these factors could have influenced the results of image matching in our study site, where 13.9% of the aerial photographs failed in the camera alignment process. One feasible suggestion to improve the completeness performance is evaluating whether increased forward overlap of up to 90% (although many recommendations suggest 80% forward overlap) could improve image matching success and accuracy in forest environment. Ginzler and Hobi (2015) demonstrated a success of creating digital surface model with a resolution of 1 m for the entire country of Switzerland with 97.9% completeness using push-broom camera of ADS40/ADS80 with 50% sidelap. In this study, the forward overlap and sidelap were estimated between 55 to 70% and 45 %, respectively which may affected the completeness of the image matching process.

The major potential of using aerial photographs in estimating and monitoring aboveground biomass are due to several factors such as high performance of estimation similar to the performance using ALS dataset, cost-effective and full automation capability in deriving the SfM dataset. The difference of RMSE value in estimating AGB between ALS and SfM datasets was less than 3% and similar result was also found in Ota et al. (2015). Digital photogrammetry is relatively cost-effective in comparison to ALS or airborne InSAR technology. For instance, Leberl et al. (2010) reported that the effective strip width for aerial photography is up to 5 times the effective width for ALS, and that aircraft can be flown at 2.5 times the speed, thus the time or cost of flight mission can be reduced significantly up to 8%. First countrywide digital surface model with a resolution of 1 × 1 m using aerial photographs is published by Ginzler and Hobi (2015) for the entire country of Switzerland, approximately 4 million hectares. Thus, given the availability of regular flight mission of aerial photographs acquisition, it is possible to derive SfM dataset for the entire country. However, one of the major concern when using SfM dataset is the incapability to detect forest floor or DTM especially in dense forest such as in tropical rainforest. Therefore, the availability of accurate DTM derived from ALS is important for full application of SfM dataset in tropical rainforest. This study used higher spatial resolution (i.e. 10 cm) of aerial photographs compared to the conventional spatial resolution used in national aerial photographs acquisition with typical resolution of 25 cm or 50 cm (e.g. Ginzler and Hobi, 2015). Thus, it is important to evaluate the influence of using lower spatial resolutions (e.g. 25 cm or 50 cm) in estimating aboveground biomass.

5. SUMMARY

The findings in this study demonstrated the capability of SfM datasets derived from aerial photographs in estimating aboveground biomass similar to the performance using ALS dataset in tropical montane forest. The difference of relative RMSE of the AGB estimation between ALS (RMSE%=32.41%) and SfM (RMSE%=35.09%) datasets was 2.68%. Thus, SfM dataset is potentially used for monitoring aboveground biomass given the availability of regular countrywide flight mission in acquiring aerial photographs and accurate digital terrain model (DTM) derived from airborne laser scanning (ALS).

ACKNOWLEDGEMENT

This research project was supported by the Advanced Carbon Monitoring in Asian Tropical Forest by High Precision Remote Sensing Technology project of the Ministry of Agriculture, Fishery and Forestry (MAFF), Japan. We are thankful to Sabah Forestry Department (SFD) for the permission, to Sabah Forest Industries (SFI) and villagers of Kampung Long Mio for the field support.

REFERENCES

Agisoft, 2014. Agisoft PhotoScan User Manual Professional Edition, Version 1.1. Retrieved July 31, 2015 from http://www.agisoft.com

Bohlin, J., Wallerman, J., and Fransson, J.E.S., 2012. Forest variable estimation using photogrammetric matching of digital aerial images in combination with a high-resolution DEM. Scand. J. For. Res., 27, pp. 692–699.

Dobson, M.C., Ulaby, F.T., Le Toan, T., Beaudoin, A., Kasischke, E.S., and Christensen, N.L., 1992. Dependence of radar backscatter on conifer forest biomass. IEEE Trans. Geosci. Rem. Sens. 30, pp. 412–415.

Eckert, S., 2012. Improved Forest Biomass and Carbon Estimations Using Texture Measures from WorldView-2 Satellite Data. Remote Sens., 4, pp. 810–829.

Fassnacht, F.E., Hartig, F., Latifi, H., Berger, C., Hernández, J., Corvalán, P. and Koch, B., 2014. Importance of sample size , data type and prediction method for remote sensing-based estimations of aboveground forest biomass. Remote Sens. Environ., 154, pp. 102–114.

Fujita, T., Itaya, A., Miura, M., Manabe, T. and Yamamoto, S., 2003. Canopy structure in a temperate old-growth evergreen forest analyzed by using aerial photographs. Plant Ecol. 168, pp. 23–29.

Ginzler, C. and Hobi, M., 2015. Countrywide stereo-image matching for updating digital surface models in the framework of the Swiss national forest inventory. Remote Sens., 7, pp. 4343–4370.

Gobakken, T., Bollandsås, O.M. and Næsset, E., 2015. Comparing biophysical forest characteristics estimated from photogrammetric matching of aerial images and airborne laser scanning data. Scand. J. For. Res., 30, pp. 73-86.

Hirata, Y., Tabuchi, R., Patanaponpaiboon, P., Poungparn, S., Yoneda, R. and Fujioka, Y., 2014. Estimation of aboveground biomass in mangrove forests using high-resolution satellite data. J. For. Res., 19, 34–41.

Ioki, K., Tsuyuki, S., Hirata, Y., Phua, M.-H., Wong, W.V.C., Ling, Z.-Y., Saito, H. and Takao, G., 2014. Estimating above-ground biomass of tropical rainforest of different degradation levels in Northern Borneo using airborne LiDAR. For. Ecol. Manage., 328, pp. 335–341.

IPCC, 2014. Climate Change 2014: Synthesis Report. Contribution of Working Groups I, II and III to the Fifth Assessment Report of the Intergovernmental Panel on Climate Change [Core Writing Team, R.K. Pachauri and L.A. Meyer (eds.)]. IPCC, Geneva, Switzerland, 151 pp.

Koch, B., 2010. Status and future of laser scanning, synthetic aperture radar and hyperspectral remote sensing data for forest biomass assessment. ISPRS J. Photogramm. Remote Sens., 65, pp. 581–590.

Leberl, F., Irschara, A., Pock, T., Meixner, P., Gruber, M., Scholz, S. and Wiechert, A., 2010. Point clouds: Lidar versus 3D vision. Photogramm. Eng. Remote Sensing., 76, pp. 1123–1134.

Müller, J., Gärtner-Roer, I., Thee, P. and Ginzler, C., 2014. Accuracy assessment of airborne photogrammetrically derived high-resolution digital elevation models in a high mountain environment. ISPRS J. Photogramm. Remote Sens., 98, pp. 58–69.

Næsset, E., 1997. Determination of mean tree height of forest stands using airborne laser scanner data. ISPRS J. Photogramm. Remote Sens., 52, pp. 49–56.

Nex, F. and Remondino, F., 2014. UAV for 3D mapping applications: a review. Appl. Geomatics, 6, pp. 1–15.

Nurminen, K., Karjalainen, M., Yu, X., Hyyppä, J. and Honkavaara, E., 2013. Performance of dense digital surface models based on image matching in the estimation of plot-level forest variables. ISPRS J. Photogramm. Remote Sens., 83, pp. 104–115.

Okuda, T., Suzuki, M., Numata, S., Yoshida, K., Nishimura, S., Adachi, N., Niiyama, K., Manokaran, N. and Hashim, M., 2004. Estimation of aboveground biomass in logged and primary lowland rainforests using 3-D photogrammetric analysis. For. Ecol. Manage., 203, pp. 63–75.

Ota, T., Ogawa, M., Shimizu, K., Kajisa, T., Mizoue, N., Yoshida, S., Takao, G., Hirata, Y., Furuya, N., Sano, T., Sokh, H., Ma, V., Ito, E., Toriyama, J., Monda, Y., Saito, H., Kiyono, Y., Chann, S. and Ket, N., 2015. Aboveground Biomass Estimation Using Structure from Motion Approach with Aerial Photographs in a Seasonal Tropical Forest. Forests, 6, pp. 3882–3898.

Phua, M.H. and Saito, H., 2003. Estimation of biomass of a mountainous tropical forest using Landsat TM data. Can. J. Remote Sens., 29, pp. 429–440.

Rahlf, J., Breidenbach, J., Solberg, S., Næsset, E. and Astrup, R., 2014. Comparison of four types of 3D data for timber volume estimation. Remote Sens. Environ., 155, pp. 325–333.

Remondino, F., Spera, M.G., Nocerino, E., Menna, F. and Nex, F., 2014. State of the art in high density image matching. Photogramm. Rec., 29, pp. 144–166.

Sabah Biodiversity Conservation Project (SBCP), 1998. Identification of potential protected areas: Ulu Padas final report. Ministry of Culture, Environment and Tourism Malaysia. pp. 123.

Thapa, R.B., Watanabe, M., Motohka, T. and Shimada, M., 2015. Potential of high-resolution ALOS–PALSAR mosaic texture for aboveground forest carbon tracking in tropical region. Remote Sens. Environ., 160, pp. 122–133

UNFCCC, 2005. Eleventh session of the Conference of the Parties (COP 11), November 2005, Montreal, Canada.

UNFCCC, 2007. Thirteenth session of the Conference of the Parties (COP 13), December 2007. Bali, Indonesia.

UN-REDD, 2013. National Forest-Monitoring Systems: Measurement, Reporting and Verification (M & MRV) in the Context of REDD+ Activities. Rome: Food and Agricultural Organization.

Vastaranta, M., Wulder, M.A., White, J.C., Pekkarinen, A., Tuominen, S., Ginzler, C., Kankare, V., Holopainen, M., Hyyppä, J. and Hyyppä, H., 2013. Airborne laser scanning and digital stereo imagery measures of forest structure: comparative results and implications to forest mapping and inventory update. Can. J. Remote Sens., 39, pp. 382–395.

Wong, W., Tsuyuki, S., Ioki, K., Phua, M.H. and Takao, G., 2015. Forest biophysical characteristics estimation using digital aerial photogrammetry and airborne laser scanning for tropical montane forest. In: 36th Asian Conference on Remote Sensing 2015., Manila, Philippines, pp. 10.

Wong, W., Tsuyuki, S., Ioki, K. and Phua, M.H., 2014. Accuracy assessment of global topographic data (SRTM & ASTER GDEM) in comparison with lidar for tropical montane forest. in: 35th Asian Conference on Remote Sensing 2014, Nay Pyi Taw, Myanmar, pp. 6.

Yamakura, T., Hagihara, A., Sukardjo, S. and Ogawa, H., 1986. Aboveground biomass of tropical rain forest stands in Indonesian Borneo. Vegetatio, 68, pp. 71–82.